The Transmembrane Domain of the Acetylcholine Receptor: Insights from Simulations on Synthetic Peptide Models

Leonor Saiz*† and Michael L. Klein*

*Center for Molecular Modeling, Chemistry Department, University of Pennsylvania, Philadelphia, Pennsylvania 19104; and †Computational Biology Center, Memorial Sloan-Kettering Cancer Center, New York, New York 10021

ABSTRACT We have studied the structure and properties of a bundle of α-helical peptides embedded in a 1,2-dimyristoyl-3-phosphatidylcholine phospholipid bilayer by molecular dynamics simulations. The bundle of five transmembrane δM2 segments constitutes the model for the pore region of the nicotinic acetylcholine receptor, which is the neurotransmitter-gated ion-channel responsible for the fast propagation of electrical signals between cells at the nerve-muscle synapse. The δM2 segments were shown to oligomerize in biomembranes resulting in ion-channel activity with characteristics similar to the native protein, and the structure of the isolated peptides was studied in 1,2-dimyristoyl-3-phosphatidylcholine bilayers and micelles by NMR experiments (Opella, S. J., et al. 1999. *Nat. Struct. Biol.* 6:374–379). Our analyses indicate that the structure, helix tilt, and the overall shape of the channel are in good agreement with the NMR experiments and the proposed model for the channel, which we show is formed by rings of functional residues. The studied geometry resulted in a closed pore state, where the channel is partially dehydrated at the hydrophobic extracellular half and the extracellular mouth of the channel blocked by the hydrocarbon chains of Arg^+ residues. The arginine amino acids form intermolecular salt-bridges with the C-terminus, which contribute as well to the bundle stabilization.

INTRODUCTION

The nicotinic acetylcholine receptor (nAChR) is the neurotransmitter-gated ion-channel responsible for the rapid communication between cells at the nerve-muscle synapse and the brain (Changeux, 1993; Hille, 1992; Karlin and Akabas, 1995; Montal, 1995; Toyoshima and Unwin, 1988). At the chemical synapses, the acetylcholine neurotransmitter molecules are released from the presynaptic membrane of an excited cell to the synaptic cleft, where the molecules diffuse to the postsynaptic membrane of the neighboring cell. The postsynaptic membrane is rich in nAChRs that specifically bind the acetylcholine neurotransmitters. The binding of two acetylcholine molecules to the extracellular ligand-binding domain of the receptor triggers a conformational change on the glycoprotein complex (Grosman et al., 2000) that opens transiently the cation-permeable ion-channel located in the cell membrane. The flow of cations through the receptors rapidly depolarizes the postsynaptic membrane, and the signal is propagated along the electrically excitable membrane toward the next nerve cell.

Among the family of the ligand-gated ion-channels, the nAChR is the best characterized (Changeux, 1993; Hille, 1992; Karlin, 2002). Structurally, it is a large glycoprotein complex (molecular mass of ~290 KDa and ~2,380 amino acids) composed by five separate polypeptide chains with stoichiometry $\alpha_2\beta\gamma\delta$ (Corringer et al., 2000; Hille, 1992; Karlin, 2002). The two α-subunits have the same amino acid sequence and contain the ACh binding sites at the extracellular side. The other subunits have homologous sequences. Each of the five subunits has four hypothesized hydrophobic transmembrane regions (M1–M4), a large extracellular domain formed by the N-terminal half of the molecule, and a substantial cytoplasmic domain formed by the loop between M3 and M4. The membrane domain has high sequence similarity among this gene superfamily which encompasses receptors for the major inhibitory neurotransmitters glycine and gamma aminobutyric acid. The different subunits are arranged in a pentameric structure around the channel and, at the transmembrane domain, all the subunits are in contact with the membrane lipid (Hille, 1992; Unwin, 1993). The M2 segments of each subunit are of particular interest since they are theorized to participate in the inner wall of the channel-forming domain confined to the membrane (Akabas et al., 1994).

The early structure of the *Torpedo marmorata* nAChR, determined by cryo-electron microscopy (EM) at a resolution of 9 Å together with image reconstitution (Unwin, 1993), provided a view of the shape of the complex, the arrangement of the subunits, some secondary structural features, and an early model in which the protein walls of the channel arranged around the aqueous pore were formed by a bundle of five amphipathic M2 α-helices, each contributed by one subunit of the pentamer, whereas the rest of the segments were relatively structureless (Unwin, 1995).

In this early picture proposed by Unwin and co-workers, the M2 α-helices were kinked in the close state of the channel at the central Leu residues (Unwin, 1993, 1995). This ring of five aligned Leu residues was suggested to constitute the gate of the channel. A 15° rotation of the M2 segments from the closed state conformation is consistent with the dimensional changes observed upon pore opening

Submitted July 22, 2004, and accepted for publication November 8, 2004.

Address reprint requests to Leonor Saiz, E-mail: leonor@sas.upenn.edu or leonor@cbio.mskcc.org.

0006-3495/05/02/959/12 $2.00

doi: 10.1529/biophysj.104.049726

(Unwin, 2003). This twisting would destabilize the gate and stabilize an open structure of the M2 bundle (Miyazawa et al., 2003). Similar large scale motions as opening mechanisms have been recently proposed for other ion-channels (Jiang et al., 2002a). Another important structural feature affecting the functioning of the nAChR are three rings of negatively charged amino acids, namely, the extracellular, intermediate, and cytoplasmic rings. These rings are involved in charge selectivity (Changeux, 1993; Corringer et al., 2000; Karlin, 2002) and, interestingly, mutations around and at the intermediate ring reducing the charge of the amino acids in neuronal α7 AChRs convert the channel ionic selectivity from cationic to anionic (Corringer et al., 1999; Galzi et al., 1992). Narrow lateral openings of a central vestibule in the intracellular domain have been also shown to act as electrostatic filters for the ions (Kelley et al., 2003; Unwin, 2003). These elements constitute the structural and functional features of the ion-channel.

Even though a variety of experimental techniques, in addition to EM, such as spectroscopic methods, information from chemical probes, and effects of mutagenesis (see the excellent recent review by Karlin, 2002), have been applied to the study the structure of the nAChR and considerable improvement of the understanding of the receptor has been reached (a number of review articles have recently appeared on the nAChR (Barrantes, 2003; Itier and Bertrand, 2001; Karlin, 2002; Leite and Cascio, 2001; Unwin, 2003)), a high-resolution structure of the receptor has been lacking. Interestingly, the recently solved structure of the snail ACh-binding protein (Brejc et al., 2001), a homologous protein, has shed light onto the extracellular domain of the nAChR, i.e., the ACh binding site. In addition, the latter and more detailed structure of the transmembrane domain of the closed receptor from the recent EM at better 4 Å resolution confirms the location of the gate, the arrangement of the inner ring of M2 α-helical segments, and the middle and outer ring of M1 and M3 and M4 segments, respectively, and suggests their secondary α-helical structure (Miyazawa et al., 2003). In particular, the kink of the M2 segments proposed at the central Leu residues from the EM experiments at 9 Å resolution (Unwin, 1993, 1995) turned out to be a slightly bent structure in this new and closer (4 Å) look at the transmembrane domain of the nAChR in the closed state of the channel (Miyazawa et al., 2003; Unwin, 2003). Moreover, the 2.7 Å crystal structure of the snail ACh-binding protein was successfully mapped into the electron densities of the nAChR extracellular ligand-binding domain. The advantage of the EM experiments is that they probe the receptors in their natural environment, since they were performed in AChR tubular crystals grown from the postsynaptic membranes of the *T. marmorata* electric organ. These samples are helical assemblies of protein and lipid molecules. Thus, even though the latest structure of the nAChR determined by cryo-EM has lower resolution than that of the recent x-ray series of images from a voltage dependent K^+ channel (Doyle et al., 1998), the former are captured in the receptor natural environment, whereas the latter probed the Fab-KvAP complexes (parts of antibody molecules—the so-called Fab fragments—were used as a scaffold to help crystallization) and lack a lipid component. The interplay between membrane proteins and, in particular, ion-channels and their natural environment is becoming more evident and, thus, the importance of lipid-protein interactions (Andersen et al., 1998; Bloom, 1998; Brown, 1994; Hilgemann, 2004; Valiyaveetil et al., 2002).

Despite the fundamental role played by the nAChR and other ion-channels and channel proteins, such as pore channels, in biology (Agre and Kozono, 2003; MacKinnon, 2003; Unwin, 2003), the structural motifs associated with function are just starting to emerge (Berneche and Roux, 2001; Changeux, 1993; Doyle et al., 1998; Hille, 1992; Oiki et al., 1988; Unwin, 1995). Precisely because of the difficulty of crystallizing membrane-embedded proteins, just a handful of high-resolution, mainly x-ray, structures are available (Bass et al., 2002; Chang et al., 1998; Doyle et al., 1998; Dutzler et al., 2002; Jiang et al., 2002a, 2002b; Kuo et al., 2003; Miyazawa et al., 2003).

Another approach to investigate structure-function relationships in these large and complex systems is to devise simplified synthetic models (bio-inspired or de novo protein design) that retain most of the functional properties of the native system (Lear et al., 1988; Montal, 1995). These minimalistic models have been proven to be especially useful in experiments and modeling investigations of large ion-channel protein complexes, such as the influenza virus M2 proton channel protein, the Virus protein U membrane protein encoded by the HIV-1 virus, the transmembrane segments of the nAChR and the glutamate NMDA receptor ion-channels (Montal, 1995). In addition, peptide assemblies have been successfully designed from first principles (de novo) to achieve the desired functioning, such as ion-channel activity (Lear et al., 1988). In the case of the nAChR, for instance, a synthetic 25-residue peptide that mimics the sequence of the hypothesized pore-lining M2 segment of the *Torpedo californica* AChR receptor δ-subunit was found to form discrete ion-channels in phosphatidylcholine bilayers (Oiki et al., 1988; Opella et al., 1999). In contrast, peptides following the sequences of the M1, M3, and/or M4 segments did not result in ion-channel activity nor did peptides with a random sequence of the M2 amino acids. The oligomerization of the δM2 transmembrane α-helical domains in model membranes resulted in ion-channel activity with characteristics, such as conductance and selectivity, not identical but similar to those of the native receptor (Oiki et al., 1988; Opella et al., 1999). Solution NMR experiments on micelle samples and solid-state NMR experiments on lipid bilayers explored the structure of the synthetic peptides in these membrane mimetic environments. The M2 segments were found to be fully α-helical with no kinks and inserted in the lipid bilayer forming a tilt angle of 12° with respect to the membrane normal. The NMR experiments together with

energetic considerations (Oiki et al., 1988) provided a model for the open state of the channel of the pore-forming peptides as a pentameric bundle of the δM2 synthetic segments. The proposed model displayed a funnel-like architecture with the wide opening located on the N-terminal intracellular side (Opella et al., 1999).

The last decade has yield revolutionary advances in computer technology that together with the development of state-of-the-art simulation methodologies have permitted the emergence of computer simulation as a powerful tool in biomembrane studies (Berneche and Roux, 2001; Law et al., 2000, 2003; Pastor et al., 2002; Roux, 2002; Saiz and Klein, 2002; Saiz et al., 2002, 2004; Tajkhorshid et al., 2002; Zhong et al., 1998, 2000). Recent molecular dynamics (MD) simulations have proved their ability to study membrane-embedded proteins in their natural environment with full atomic detail (Berneche and Roux, 2001; Tajkhorshid et al., 2002). Minimalistic designed models of ion-channels consisting of pore forming bundles of α-helical peptides, one of the typical motifs on ion-channel pores, have been the focus of attention of atomistic MD simulations (Law et al., 2000, 2003; Saiz et al., 2002, 2004; Zhong et al., 1998, 2000) due to the manageable system size compared, for instance, to the 290 KDa native nAChR.

We have recently studied the properties of a model membrane with the homopentameric bundle of the δM2 segments of the nAChR designed by Montal and co-workers at similar conditions as those of the NMR experiments (Opella et al., 1999) by performing fully atomistic MD simulations (Saiz and Klein, 2002; Saiz et al., 2002, 2004). The peptides contain all the structural features related to function important for the nAChR, such as the negatively charged intermediate ring (selectivity) and the central leucine residues (gate), and have been shown to form functional pores in 1,2-dimyristoyl-3-phosphatidylcholine (DMPC) lipid bilayers with ion-channel activity similar to that of the native receptor (Oiki et al., 1988; Opella et al., 1999). The peptide bundle was embedded in a fully hydrated DMPC lipid bilayer in the biologically relevant fluid lamellar phase, L_α. The previous work focused on the influence of the pore forming bundle on the physical properties of the phospholipid bilayer, and we identified important lipid-peptide interactions or complexes, specifically, interactions of the external Lys amino acids with the lipid headgroup phosphate groups (Saiz et al., 2004). Snorkeling of Lys^+ residues to make contact with lipid headgroups is generally observed in experiments on membrane peptides and proteins (Killian, 2003). We explore here the structure of the peptide bundle and its functional properties and compare the results of the analyses with the available experimental data.

METHODS

The molecular model of the pore region of the nAChR ion-channel we have studied was designed from NMR experiments and energy considerations on functional synthetic peptides (Oblatt-Montal et al., 1993; Oiki et al., 1988; Opella et al., 1999; Montal, 1995). The model consists of the transmembrane homopentameric bundle of the α-helical M2 segments of the glycoprotein. These M2 segments correspond to the δ-subunit of the native nAChR of the *Rattus norvegicus* and are characterized by the following sequence: GSEKMSTAISVLLAQAVFLLLTSQR, where residues G- and -R constitute the N- and C-terminal, respectively. From the folding of the natural protein, the two termini are assigned to the intracellular or cytoplasmic (N) and extracellular or synaptic side of the membrane (C) (Hille, 1992). The amino acid side chain ionizable states were chosen appropriately to the pH used in the NMR experiments of the M2 segments in lipid bilayers (pH 7.4, which corresponds to physiological conditions) and the N- and C-terminus were protonated and deprotonated, respectively (Opella et al., 1999).

The peptide bundle was embedded in a fully hydrated DMPC lipid bilayer in the biologically relevant fluid lamellar phase, L_α. The system contained 23349 atoms and was constituted by 5 peptides, 47 DMPC lipid molecules per monolayer (lipid to peptide molar ratio of 19:1), 5 chloride (Cl^-) counterions, and 3434 water molecules. The initial coordinates for the α-helical M2 segments correspond to one of the 10 minimum energy configurations of the 1A11 entry (Opella et al., 1999) in the PDB (specifically, the 10th configuration). In Fig. 1, we show a snapshot of the simulated system where only the molecules located within the simulation cell are depicted.

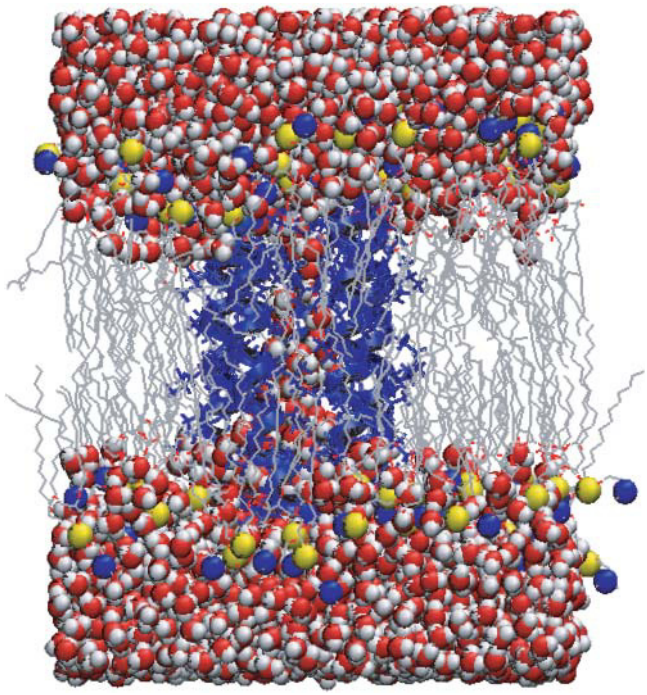

FIGURE 1 Configuration of the system taken from the MD simulation after 4.5 ns. Only the molecules within the central simulation cell are shown. The lipid molecules are shown as sticks except for the N and P atoms of the headgroups, which are displayed as blue and yellow spheres, respectively, and the hydrogen atoms, which are not shown. The atoms of the water molecules are represented as white (hydrogen) and red (oxygen) spheres. The M2 helices are shown in blue with the backbone as ribbons and the side chains as sticks. The radii of the spheres correspond to the atomic van der Waals radii of the different species. The N-terminus (intracellular) is located at the bottom of the bundle. The unit cell dimensions are $L_x = 55.2 \pm 0.6$ Å ($1\ \text{Å} = 10^{-10}$ m; all errors are given as standard deviations), $L_y = 55.8 \pm 0.9$ Å, and $L_z = 71 \pm 1$ Å, where the *x*-*y* plane corresponds to the plane of the interface and the *z* axis is parallel to the membrane normal.

In the initial configuration, the synthetic amphipathic peptides were arranged as a symmetric pentamer, separated by ~12 Å, and had their main axis oriented perpendicularly to the membrane surface. The hydrophilic residues of the helices were arranged facing the pore interior and the hydrophobic ones facing the lipids. Specifically, residues Glu-3, Ser-6, Ser-10, Val-17, Leu-20, and Gln-24 were initially (on average) exposed to the pore lumen in agreement with mutagenesis, affinity labeling, and cysteine-accessibility measurements on the heteropentameric receptor (Akabas et al., 1994; Karlin, 2002; Opella et al., 1999). The pentameric bundle was then inserted in a preassembled fully hydrated DMPC lipid bilayer containing 128 lipid molecules and a water to lipid ratio of 28:1. It has been shown previously that at the same conditions, a smaller pure DMPC lipid bilayer with a slightly reduced number of water molecules to match the hydration used in structural experiments, gives properties, such as area per lipid, interlamellar spacing, deuterium order parameter profiles, and average orientation of headgroup dipole moments, in excellent agreement with experiments (Bandyopadhyay et al., 2001; Saiz et al., 2004). Upon insertion, overlapping water and lipid molecules close to the peptide bundle were removed, giving rise to the empty cylinder occupied by the pore-forming bundle structure. The interior of the pore was hydrated initially by a column of water molecules. In the final system, the number of lipid molecules was thus reduced from 128 to 94 with the same number of lipids in each monolayer, and the number of water molecules reduced from 3584 to 3439 and further to 3434 after transforming five water molecules into counterions to preserve electroneutrality.

Following standard procedures, the equilibration of the system consisted of a short series of classical MD simulations at constant temperature (T = 303 K) and volume (NVT ensemble) to minimize the van der Waals interactions between the different pieces of the constructed system. The atoms of the peptides and water molecules inside the pore were fixed during an additional 400 ps NVT simulation run to ensure that the lipid (and water) molecules were able to rearrange properly around the cylindrical protein inclusion. The system was then relaxed from the imposed constraints and the simulation run for another 100 ps in the NVT ensemble. The equilibration period was completed by an MD simulation of ~2 ns at constant temperature and pressure, P = 1 atm (1 atm = 101.3 kPa), (NPT ensemble). Classical MD simulations were then performed at constant temperature, T = 303 K, and pressure, P = 1 atm, for another 5 ns, completing a total of more than 7.5 ns. All the simulations were performed with the usual periodic boundary conditions.

For the equilibrium simulations and the last stage of equilibration, we used the Nosé-Hoover thermostat chain extended system isothermal-isobaric dynamics method, as implemented in the program PINY_MD (Tuckerman et al., 2000), with an orthorhombic simulation cell and a reversible multiple time step algorithm (Tuckerman et al., 1992). After equilibration, different properties were evaluated over the production run of 4.5 ns unless otherwise stated.

The molecular and potential model used for the different components of the biomembranes was the recent version of the all-atom CHARMM force field (Feller and MacKerell, 2000; MacKerell et al., 1998; Schlenkrich et al., 1996) and the rigid TIP3P model for water (Jorgensen et al., 1983). During the simulations, all the motions involving hydrogen atoms were frozen. The short-range forces were computed using a cutoff of ~10 Å, and the minimum image convention and the long-range forces were properly (Patra et al., 2003; Tobias, 2001) taken into account by means of the particle mesh Ewald technique (Darden et al., 1993).

RESULTS AND DISCUSSION

Peptide structure

The early EM map at 9 Å resolution suggested that the M2 rods were kinked around the central Leu-251 (Leu-13 in the sequence order used here) where the gate of the channel was located and the loss of α-helicity was affecting both the open and the closed conformations of the receptor (Unwin, 1993, 1995). This secondary structure contrasts with the NMR experiments of the individual (isolated) δM2 and αM2 segments in membrane mimetic environment (Opella et al., 1999; Pashkov et al., 1999) and the recent EM densities at 4 Å resolution where no kinks are present (Miyazawa et al., 2003; Unwin, 2003). In the case of the synthetic δM2 peptides used in this study as the initial configuration, the structure of the 10 lowest energy configurations determined by solution NMR in dodecylphosphocholine micelles is characterized by fully α-helical backbones whose structures superimpose quite well, especially between residues Lys-4 and Gln-24 (Opella et al., 1999; Montal and Opella, 2002).

To get insights into the stability and structure of the peptides and their secondary structure in the lipid bilayer during the time scale of the simulations, we calculated the standard Φ and Ψ torsional angles of the peptide backbones for the five M2 membrane spanning peptides on average and as a function of time (Stryer, 1995). The Ramachandran plots (data not shown) indicate that the values correspond mainly to right-handed α-helices lying in the region of $\Phi \sim -57°$ and $\Psi \sim -47°$, except for the end residues at both N- and C-terminus, which diverge from the α-helical conformation. In Fig. 2, we show the average values of Φ (*black*) and Ψ (*red*) angles for the individual residues of each of the five peptides. The backbone angles for the initial NMR configuration are also included (*solid symbols*) for comparison. The values for the Φ and Ψ angles are approximately uniform along the peptide, except for those residues outside the 3–23 range. This confirms that the points lying outside the right-handed α-helical region of the Ramachandran plot correspond to residues located at the peptide ends. In addition, the region around Leu-13 does not show any deviation from the standard values for α-helical secondary structure. This was also confirmed when the hydrogen bonding (HB) structure between N-H and C=O pairs in n and n ± 4

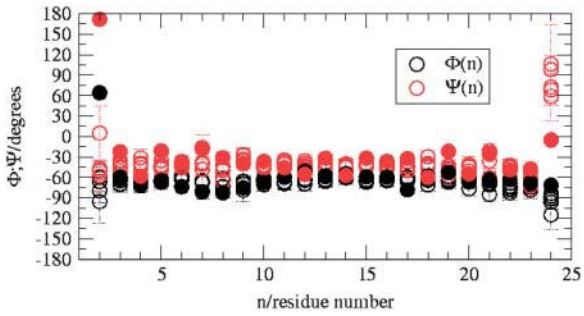

FIGURE 2 Average values of Φ (*black open symbols*) and Ψ (*red open symbols*) peptide backbone angles for the five peptides as a function of the position of the residues from Ser-2 to Gln-24. The error bars were calculated for each M2 segment as the standard deviations (during the last 4.5 ns of the simulations). The values for the initial NMR configuration [Φ (*black solid symbols*) and Ψ (*red solid symbols*)] used are also plotted.

residues was evaluated. Visual inspection indicates that the M2 segments can be slightly bent. Interestingly, it seems that the values for the initial NMR configuration (*solid symbols* in Fig. 2) heal during the simulation tending to be closer to the expected values for α-helices.

Peptide transmembrane positioning

Our analyses show that ~21 of the 25 residues maintain the α-helicity during the simulations. This can be understood in terms of the position of the different residues along the direction normal to the membrane (z) and lipid-water interface.

A useful way to quantify the position along the bilayer normal of the different membrane components is by characterizing the density profiles normal to the bilayer surface, which can be measured experimentally by neutron and x-ray scattering. The electron density profiles (EDPs), which can be computed for each atomic and/or molecular species, are proportional to the density profiles obtained by x-ray scattering experiments at low angles (White and Wiener, 1992). In Fig. 3, we plot the average EDPs as a function of z obtained for the different molecular components of the system, namely, water, lipid molecules, and peptides. Note that the center of the membrane is located at $z = 0$ Å, and negative values of z correspond to the intracellular side of the membrane. The peptides span the lipid bilayer, in particular the hydrophobic length of the membrane, specified by the region between the two glycerol distributions in Fig. 3 and have their extremes located at the wide lipid-water interfaces. The interfaces are characterized by the overlapping distributions of water and lipid molecules. At these two regions, lipid headgroups (shown in Fig. 3 as the distributions of phosphate and choline groups) and water molecules interact with each other and with the peptide ends.

The average position along z of the different peptide residues is shown in Fig. 4. The M2 peptides are capped at both ends by polar and charged residues at positions along the membrane normal that lie within each of the two membrane interfaces, i.e., within and above the position of the lipid glycerol groups. The results of our analysis indicate that, at the membrane interface, competing interactions take place, in contrast to what happens in the hydrophobic region of the lipid bilayer where α-helical structures are energetically more favorable. The backbone N-H and C=O groups of the end residues can form HBs with water, the oxygen atoms of the lipid headgroups and interact with the choline group (Figs. 3 and 4), which will compete with the backbone N-H···O=C HBs and thus will lead to a loss of backbone secondary structure.

Fig. 4 evidences the presence of rings of amino acids one contributed by each of the M2 peptides. In the natural receptor, the residues are not always identical, but the rings are formed by homologous amino acids.

Bundle structure and pore shape

In the initial conformation, the transmembrane amphiphilic peptides were oriented with their main axes parallel to the bilayer normal and forming a pentamer with the residues Glu-3, Ser-10, Val-17, Leu-20, and Gln-24 (hydrophilic side of the helices) oriented toward the pore lumen (consistent with self assembly concepts of amphipathic rods). The initial pentamer was built so each segment was located at ~12 Å from the center of mass of the bundle since the size of α-helices is ~10 Å.

During the multinanosecond time scale investigated, the peptide bundle adopted a left-handed coiled coil structure.

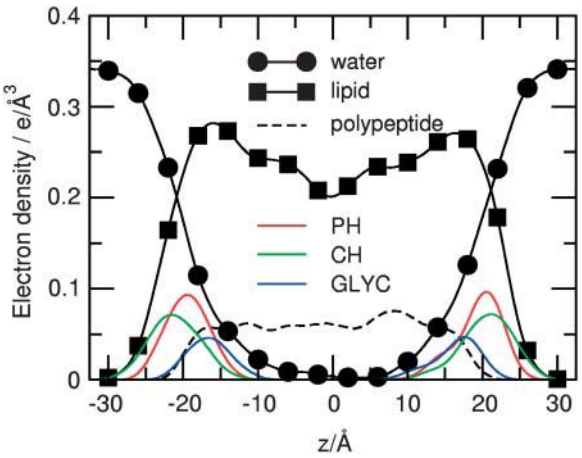

FIGURE 3 EDPs of the different molecular species (water, lipids, and peptides) along the membrane normal (z). For the lipid molecules, the contributions due to the phosphate (PH) and choline (CH) groups of the headgroups and the glycerol (GLYC) backbone are also shown. Negative z values correspond to the intracellular side of the membrane.

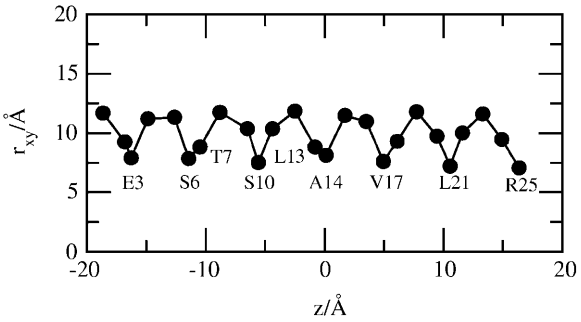

FIGURE 4 Average position of the C_α atoms of each residue with respect to the center of mass of the bundle in the x-y plane as a function of the average position of the amino acid along z (the membrane normal). Only the residues closer to the channel axis are indicated. Negative z values correspond to the intracellular side of the membrane. It is interesting to note that only the residues facing the pore lumen located at the intracellular side are hydrophilic (polar or charged), whereas the extracellular ones are hydrophobic, except for the last residue Arg^+ located at the extracellular entrance or mouth of the channel.

Each helix tilted with respect to the membrane normal fluctuating during the first 3 ns and adopted afterward a common average orientation of ~12°, which agrees well with the NMR data (12°) at similar conditions (Opella et al., 1999). The peptide bundle is stable during the period studied. In Fig. 5, we plot the tilt angle of the five peptides with respect to the membrane normal for the last 5 ns of the simulation, and the value obtained from the NMR experiments is included for comparison. After the first 500 ps shown in Fig. 5, all the peptide orientations fluctuate around the same mean value. During the equilibration period, the initial distance between the peptides and the bundle center of mass is reduced from 12 Å to ~10 Å (see Fig. 4, where the average distance in the *x*-*y* plane of the membrane surface with respect to the bundle center of mass is shown for each residue) and the center of mass of near neighbor helices are separated by ~11 Å. The initially parallel pentameric system, in addition to the tilt, develops a left-handed twist adopting the coiled-coil-like structure (Fig. 1) to preserve the hydrophilic interface at the pore lumen. Due to the amphiphilic character of the M2 segments, the hydrophilic residues Glu-3, Ser-6, and Ser-10 maintain their orientation facing the interior of the pore during the simulation as evidenced in Fig. 4. These characteristics, which naturally arise in these simulations, are in excellent agreement with the model proposed by Montal and co-workers (Opella et al., 1999).

In our conformation, the dipole moments of the peptides created by the aligned backbone dipoles typical of α-helical structures are aligned (as in the natural receptor) and thus a considerable dipole moment for the bundle is expected. The total dipole moment of the peptide bundle (data not shown) is basically the component along the membrane normal *z*. The initial departure from the 12° observed in the NMR experiments for the helix orientation leads to larger projection components of the total dipole moment in the membrane plane (*x* and *y*), which are reduced for the last 4.5 ns of the simulation. During these periods, the *z* component increases in absolute value and reaches ~−350 Debyes for the last 4.5 ns. It is worth noting that this value is equivalent to having for each peptide a charge of $\sim\pm 0.5\ e$, where *e* is the absolute value of the electron unit of charge, separated by ~30 Å, and, in the natural channel, the dipole moment of the M2 segments is compensated by the dipoles of the rest of the transmembrane segments (M1, M3, and M4) in each subunit. The observed evolution indicates that the structure of the bundle is still evolving toward an equilibrium configuration that is finally reached after ~3.5 ns (i.e., for the last 4.5 ns) and, thus, helix orientation and the components of the total dipole moment of the bundle are very useful to monitor the stabilization of peptide bundles.

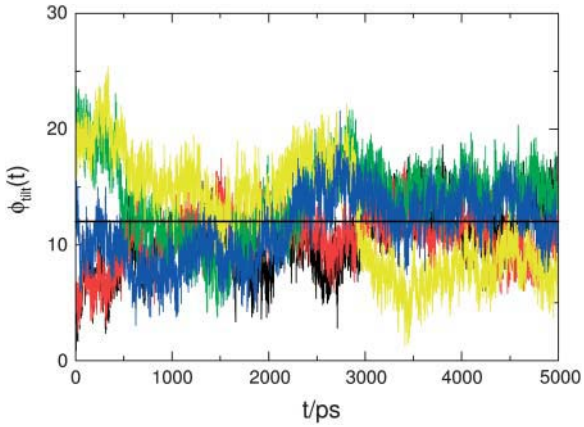

FIGURE 5 Orientation of the five M2 peptides with respect to the bilayer normal as a function of time for the last 5 ns of the simulation.

The tertiary structure of the bundle leads to a water-filled cavity and the pore interior built by rings of equal amino acids. These rings can be modulated by fluctuations and a loss of symmetry. Importantly, our results indicate that of those residues closer to the center of the bundle, and thus of those residues forming the pore walls, only one-half of them are hydrophilic. In particular, the channel is hydrophilic at the intracellular side (Fig. 4). The intracellular mouth is formed by the ring of negatively charged Glu-3 residues. Two polar serine rings (Ser-6 and Ser-10) provide a hydrophilic pore interior until the center of the bilayer is reached. The rest (extracellular half) is constituted only by hydrophobic residues (rings of Leu-13-Ala-14, Val-17, and Leu-21) spanning more than 10 Å. The extracellular mouth contains the final charged ring constituted by the arginine residue (Arg-25). Considering that the channel in the open conformation (consistent with our structure and orientation) would require the presence of water to be functional, the fact that one-half of the pore is hydrophobic would lead indeed to interesting transport phenomena.

Water and ion transport is determined not only by the structure and composition of the amino acid rings but also by the fluctuations of the helices. We have explored the dynamics of the bundle by calculating its inertia tensor. The inertia tensor has two similar large components in the plane of the membrane and a small component corresponding to the direction of the membrane normal as expected for bundles of cylindrical shape. Fluctuations of all the components take place during the time scale of the simulation. Of particular interest are the fluctuations of the two larger components which correspond to movements of the bundle in the plane of the membrane, which can be associated with breathing motions of the bundle. In Fig. 6, we plot the evolution of the inertia tensor components along the principal axes as a function of time for a 1 ns time window. These collective oscillations on the order of 200–300 ps were also observed in peptide bundles in membrane mimetic environment by MD simulations (Zhong et al., 1998).

To complement this picture and get an idea of the shape of the channel (the interior of the pore), we show in Fig. 7 the EDPs for water molecules in an appropriate scale. The

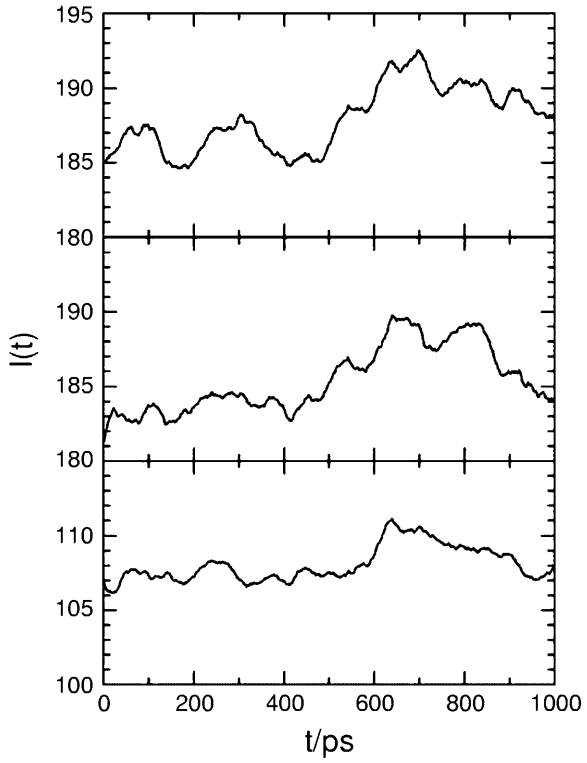

FIGURE 6 Evolution of the components of the inertia tensor, $I(t)$, of the five-helix bundle projected along the principal axes. Units are $m \times$ Å^2, where m is the unit of atomic mass.

water-filled bundle displays a funnel-like architecture with the narrow region located at the C-terminus (synaptic/extracellular) in agreement with the proposed model based on NMR experiments and energetic considerations (Opella et al., 1999). The average density of water molecules inside the channel during the last 4.5 ns depicted in Fig. 7 suggests

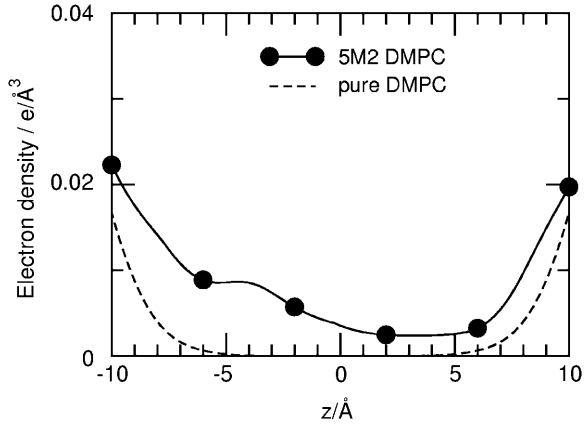

FIGURE 7 EDPs of water molecules along the membrane normal (*solid lines* and *symbols*; denoted by 5M2 DMPC). The results obtained for a pure DMPC lipid bilayer at similar conditions (Saiz et al., 2004) are included for comparison (*dashed lines*; denoted by pure DMPC).

this funnel shape for the region -7 Å $\leq z \leq 7$ Å, where the contribution to the electron density from water molecules outside the channel is not important as suggested by the comparison of the water EDPs for the pure lipid bilayer and that containing the pore-forming peptides. This average shape of the water-filled bundle (wide at the intracellular half and narrow at the extracellular half) is consistent with the hydrophilic (hydrophobic) interior associated with intracellular (extracellular) side.

Water in the pore and charged rings at the channel mouths

We have followed the evolution of the water molecules to have an instantaneous picture of the hydration of the pore. In Fig. 8, we show the position of the water molecules inside the simulation cell as a function of time for four specific instances, namely, 2.5 ns, 4.5 ns, 5.5 ns, and 7 ns. After a few nanoseconds, the column of water molecules of the initially fully hydrated interior of the bundle becomes thinner at the extracellular half until it is formed by basically a single file of water molecules that finally breaks after ~5.5 ns and leaves the channel upper interior dehydrated (Fig. 8, *right panels*). From 2.5 ns to 5.5 ns, the number of water molecules inside the channel decreases from ~60 water molecules to 30. During the whole simulation period, the half of the channel corresponding to the N-terminus (intracellular) contains water.

On the one hand, this partial dehydration is caused by the positively charged ring of arginine residues located at the extracellular mouth of the channel, which interact with the negatively charged (deprotonated) C-terminus of the neighboring helices. The formation of intermolecular $Arg^+ \cdots COO^-$ salt-bridges, which contributes significantly to the stabilization of peptide-peptide interactions in the bundle, blocks eventually the extracellular mouth due to their bulky hydrocarbon chains. On the other hand, since the extracellular half of the channel interior is lined by rings of hydrophobic residues (from Leu-13–Ala-14 to Leu-21) for more than 10 Å and the Leu-13 residues are oriented toward the interior of the pore in the simulations, the blocking of the channel by Arg-25 is accompanied by the dehydration of this region.

Perfect symmetry of the pentameric bundle would imply an intermolecular structure with formation of salt-bridges of the $Arg^+ \cdots COO^-$ type between each peptide and its near neighbors. Peptide bundles with an even number of M2 segments have more possible states. In the case of a tetrameric bundle, for instance, two states are possible: one with associated dimers and the other with a coiled coil tetrameric structure. Indeed, MD simulations of a synthetic ion-channel have reported a transition between a dimer-of-dimers and a tetrameric structure for a four helix bundle in the nanosecond time scale (Zhong et al., 1998). In our pentameric bundle, perfect symmetry may result in the

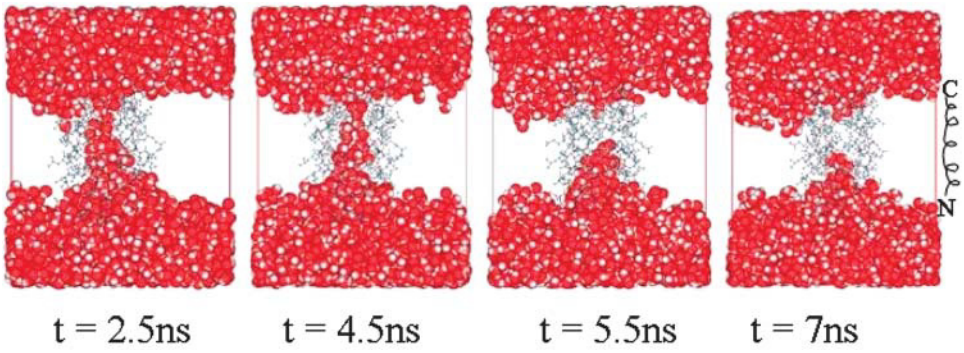

FIGURE 8 Evolution of the water molecules inside the unit cell as a function of time. The snapshots correspond to (from *left* to *right*) 2.5 ns, 4.5 ns, 5.5 ns, and 7 ns. The atoms of the water molecules are represented as white (hydrogen) and red (oxygen) spheres with radii corresponding to the atomic van der Waals radii of the different species. The M2 helices are shown as sticks. The N-terminus (intracellular) is located at the bottom of the bundles.

unblocking of the extracellular mouth of the channel. However, due to the loss of secondary structure at the ends of the peptides, there is an increased mobility of the C-termini at the extracellular side of the bundle. This leads to the formation of a salt-bridge of the $Arg^+\cdots COO^-$ type between one peptide and one of its next near neighbor. The hydrocarbon chain of the arginine residue is thus bridging the two peptide ends and blocking the channel. The other next near neighbor arginine amino acid does not form a salt-bridge, and the chain remains trapped below in the pore. This loss of perfect symmetry for the pentameric bundle is consistent with the experimental data on the channel activity of this system, where Opella and co-workers (1999) observed heterogeneous conductances and lifetimes, suggesting a number of different oligomerization states of the M2 peptides. Gating of water pores mediated by salt-bridges has also been observed in other membrane proteins, such as OmpA (Bond et al., 2002) and the glutamate receptor (Arinaminpathy et al., 2003). The salt-bridges could be slightly affected by the particular force-field used. In addition, hydration has been suggested as a possible key factor for molecular recognition of protein-DNA complexes. There, Arg^+ interacts with the phosphate group of the DNA molecule (a situation similar to our case) and ab initio calculations suggested that hydration is accompanied by significant polarization effects (Frigyes et al., 2001), which are only considered in an effective way in the used CHARMM force-field (MacKerell et al., 1998).

Recent studies of water conduction through the hydrophobic channel of a nanotube (Hummer et al., 2001) or other nanometer-sized cylindrical channels (Allen et al., 2002) have observed intermittent water transport tunned by changes in local channel polarity. Nanosecond fluctuations of water density in short hydrophobic pores of varying radii was also reported with water flow occurring in bursts as well (Beckstein and Sansom, 2003). More importantly, when a hydrophobic nanopore impermeable to water under equilibrium conditions was placed connecting two reservoirs with different Na^+ concentrations, the strong electric field created drives water molecules into the channel. Cation passages through the pore reduced the electric field, until the pore empties of water and closes (Dzubiella et al., 2004). These studies in simple models indicate that even if the channel were not blocked at the extracellular mouth by the intermolecular salt-bridges, the hydrophobic half of the channel may be dehydrated and thus effectively closed, at least for transient periods if the pore dimensions and local channel polarity are consistent with the intermittent water transport.

The results of our analyses indicate that the simulated structure corresponds to a closed state of the pore forming peptides. However, experimental measurements show channel activity of the associated M2 helices in DMPC lipid bilayers. There are two possibilities for the channel to be open. On the one hand, there could be an equilibrium between a structure of the M2 oligomers where the Arg^+ residues interact with the COO^- terminus via salt-bridges, which would correspond mostly to a closed state of the channel model as seen from our simulations, and another situation where Arg^+ residues (and the COO^- groups) are fully solvated by water molecules and thus the extracellular mouth is free, which would possibly correspond to an open structure of the M2 oligomers. Interestingly, this situation would be closer to the native channel, since the different segments M1–M4 are covalently linked and, thus, the Arg^+ residues are not at the free ends of the helices. On the other hand, one should notice that the single-channel currents were recorded under voltage clamp conditions for symmetric salt concentrations. Therefore, there is an electric field acting on the lipid bilayer and, thus, on the Arg^+ residues, which could orient the charges at the end of the long (and thus mobile) Arg^+ and open the channel (Bezanilla and Perozo, 2002). The location of the Arg^+ residues at the mouth of the channel is ideal for the charges to be oriented by the electric field. Indeed, Lys^+ and Arg^+ amino acids are usually associated with voltage sensors (Bass et al., 2002; Jiang et al., 2003a,b). Simulations of the peptide bundle under an electric field could be carried out to confirm this as a possible mechanism for opening of the channel. In addition, the presence of the electric field could drive water inside the hydrophobic (extracellular) half of the channel as observed in model systems with the electric field driving the system from a dry to a hydrated pore (Dzubiella et al., 2004).

Concerning ion charge selectivity, some insights can be obtained from the analysis of the Cl^- counterion density

distribution. In our previous study, we explored the effects of the peptide bundle on the properties of the phospholipid bilayer. In particular, we observed a shift of the average orientation of the lipid headgroup dipole moments from 70° for the pure lipid bilayer to 60° with respect to the membrane normal (Saiz et al., 2004). This trend could be understood because, after incorporating the peptide bundle, the intracellular side of the membrane has a net positive charge evident in the charge density profiles (data not shown). Therefore, the positively charged choline groups tend to be expelled from the lipid-water interface decreasing in this way the average dipole orientation angle with respect to the membrane normal. The net positive charge of the intracellular side of the membrane causes an effective attraction of the chloride counterions for this interface. This is evident in the EDP of the Cl ions, which displays a maximum at ~ -26 Å, close to the lipid headgroup choline group density (Fig. 9). A shoulder in the Cl^- EDP distribution is apparent at the (neutral) extracellular side at a similar position but slightly shifted away from the interface. The density distribution of Cl ions at the extracellular surface is in good agreement with that observed in neutral phosphatidylcholine lipid bilayers with NaCl salts, where Cl ions interacted with the choline groups but mostly conserved their hydration water (Pandit et al., 2003). In this system, the role of the negatively charged ring of Glu-3 residues at the extracellular mouth of the channel seems to be crucial for charge selectivity of the channel since the Cl^- ions are most probably located close to that membrane surface. Interestingly, the COO^- groups of the glutamic acid residues are mostly oriented in the direction of the membrane normal pointing toward the exterior of the pore (Fig. 9, *bottom panel*). In this orientation, they are ready to prevent Cl^- ion penetration into the channel, controlling the charge selectivity of the channel observed in the experiments (Opella et al., 1999).

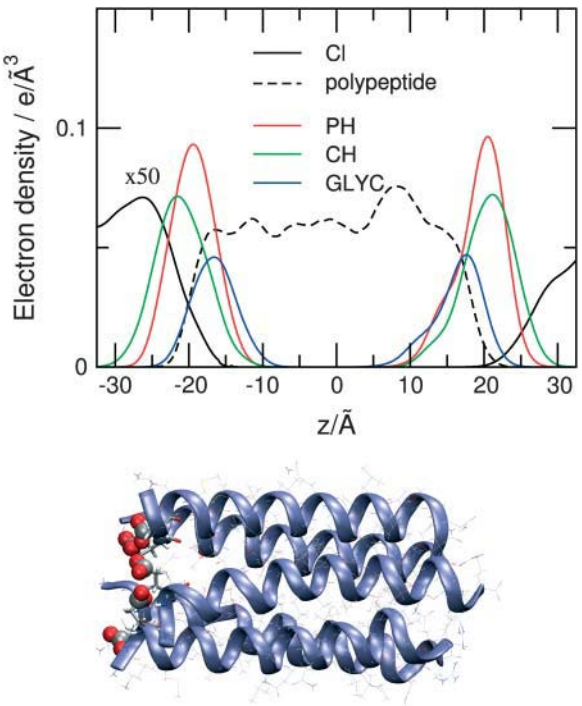

FIGURE 9 (*Top*) EDPs of counterions (augmented by a factor of 50) showing the tendency of the Cl^- atoms to remain closer to one of the membrane interfaces, the positively charged intracellular side. The negative z values correspond to the intracellular leaflet. The EDP corresponding to the peptides, the phosphate (PH) and choline (CH) groups of the lipid headgroups, and the glycerol (GL) backbone of the lipid molecules are included for clarity. (*Bottom*) Peptide bundle shown with the residues as sticks and the backbones as purplish ribbons. The ring of Glu-3 residues located at the intracellular side is highlighted by displaying the residues as thick sticks and the COO^- group as spheres in gray (C atom) and red (O atoms). The orientation of the peptide bundle is appropriate to the scale shown in the top panel. Note that the COO^- groups of the Glu-3 residues are oriented pointing toward the water phase.

CONCLUSIONS

We have explored the structure and properties of a pore forming homopentameric peptide bundle of synthetic δM2 segments in a DMPC phospholipid bilayer by MD simulations. The amphipathic δM2 peptides were designed by Montal and co-workers (Opella et al., 1999) as a minimalistic model for the pore region (with five-fold symmetry) of the nAChR ion-channel, which is the neurotransmitter-gated ion-channel responsible for the fast propagation of electrical signals between cells at the nerve-muscle synapse and the brain (Hille, 1992). Indeed, the peptides were shown to oligomerize in lipid bilayers forming functional pores with characteristics similar to those of the natural receptor, and the structure of the isolated peptides was studied by solid-state and solution NMR experiments in membrane mimetic environments (Opella et al., 1999). The results of our analyses show that the peptide bundle is stable for the multinanosecond time scale investigated. The secondary structure of the peptides remains mostly α-helical except for those residues at the end of the segments, which are located at the lipid-water interface. During the early stages of the simulations, the peptides deviate from the initial orientation parallel to the membrane normal, and the average tilt angle of 12° is in excellent agreement with the NMR experiments in DMPC lipid bilayers. In addition to the tilt, the oligomerized peptides develop a left-handed twist adopting a coiled-coil-like structure to preserve the hydrophilic interface at the pore lumen.

We have shown that this tertiary structure results in a pore formed by rings of functional residues. Rings of hydrophilic residues (Glu-3, Ser-6, and Ser-10) maintain their orientation toward the bundle center and face the interior of the pore at the intracellular (cytoplasmic) side of the channel. The rest of the pore interior is constituted by three rings of hydrophobic residues (Leu-13–Ala-14, Val-17, and Leu-21) and a charged ring of Arg^+-25 at the extracellular (synaptic) mouth of the channel.

The in-plane collective fluctuations of the components along the principal axis of the inertia tensor of the bundle, which represent breathing modes of the bundle, have been observed and are expected to be important for water and ion conduction through the rings of amino acids. The initially hydrated interior of the channel becomes dehydrated at the extracellular half due to the presence of the hydrophobic rings, and the pore is effectively closed at the extracellular channel mouth. At this mouth, interhelical salt-bridges of Arg^+ with the deprotonated COO^- terminus stabilize the peptide bundle. The lack of perfect five-fold symmetry of these interactions, which is consistent with the observed heterogeneous conductances and lifetimes of the channels indicating a number of different oligomerization states, leads to the effective closing of the channel by the bulky hydrocarbon chains of Arg^+ residues.

The conformational transition between open and closed states of the channels may be understood in terms of the experimental conditions of the channel conductance measurements. These were performed under voltage clamp conditions for symmetric salt concentrations. Therefore, there was an electric field acting on lipid bilayer, and thus on the Arg^+ residues, which could orient the charges at the end of the long (and thus mobile) Arg^+ and open the channel (Bezanilla and Perozo, 2002). Indeed, Lys^+ and Arg^+ amino acids are usually associated with voltage sensors (Bass et al., 2002; Jiang et al., 2003b). Simulations of the peptide bundle under an electric field could be carried out to confirm this as a possible mechanism for opening of the channel. In addition, the presence of the electric field could drive water inside the hydrophobic (extracellular) half of the channel as observed in model systems (Dzubiella et al., 2004).

Interestingly, the use of Cl^- counterions for charge neutralization permitted us to study their behavior close to the neutral (extracellular) and the positively charged (intracellular) membrane surfaces. The role of the negatively charged Glu^--3 ring located at the intracellular mouth of the channel is thus crucial in this system for ion charge selectivity since the Cl^- atoms are on average more attracted to the positively charged intracellular side.

It is still not clear whether the M2 helices of the natural nAChR are kinked in the open state of the channel since a high-resolution structure is still lacking (Unwin, 2003). Even though the M2 segments remain α-helical during the time scale of our simulations, one cannot rule out that a kinked conformation could be developed under tension (caused by the conformational change in the protein complex upon binding of ACh). Recently, a similar mechanism has been proposed for the K^+ ion-channels (Jiang et al., 2002a). The pore helices, which are straight in the apparently relaxed closed state of the pore, can bend in the open conformation, causing the bundle to splay open. However, usually, proline residues have a prominent role in creating kinked structures in transmembrane peptides (Sansom and Weinstein, 2000).

The results of our analysis confirm the importance of studying minimalistic protein models to get insights into structure-function relationships in large protein complexes, such as the nAChR ion-channel. Further computational studies will follow to include the rest of the transmembrane domain of the nAChR protein complex constituted by 20 α-helical TM segments, i.e., four (M1–M4) for each of the five ($\alpha_2\beta\gamma\delta$) subunits (Miyazawa et al., 2003), and possibly the extracellular ligand-binding domain of the receptor in the different states of the channel as the corresponding structures are made available from experiments.

This work has been supported by the National Institutes of Health. Computer facilities were provided by the National Center for Supercomputing Applications. Figs. 1 and 9 (*bottom*) were drawn using VMD (Humphrey et al., 1996).

REFERENCES

Agre, P., and D. Kozono. 2003. Aquaporin water channels: molecular mechanisms for human diseases. *FEBS Lett.* 555:72–78.

Akabas, M. H., C. Kaufmann, P. Archdeacon, and A. Karlin. 1994. Identification of acetylcholine-receptor channel-lining residues in the entire M2 segment of the α subunit. *Neuron.* 13:919–927.

Allen, R., S. Melchionna, and J. P. Hansen. 2002. Intermittent permeation of cylindrical nanopores by water. *Phys. Rev. Lett.* 89:175502.

Andersen, O. S., C. Nielsen, A. M. Maer, J. A. Lundæ, M. Goulian, and R. E. Koeppe. 1998. Gramicidin channels: molecular force transducers in lipid bilayers. *Biol. Skr. Dan. Vid. Selsk.* 49:75–82.

Arinaminpathy, Y., P. C. Biggin, I. H. Shrivastava, and M. S. P. Sansom. 2003. A prokaryotic glutamate receptor: homology modelling and molecular dynamics simulations of GluR0. *FEBS Lett.* 553:321–327.

Bandyopadhyay, S., J. Shelley, and M. L. Klein. 2001. Molecular dynamics study of the effect of surfactant on a biomembrane. *J. Phys. Chem. B.* 105:5979–5986.

Barrantes, F. J. 2003. Modulation of nicotinic acetylcholine receptor function through the outer and middle rings of transmembrane domains. *Curr. Opin. Drug Disc.* 6:620–632.

Bass, R. B., P. Strop, M. T. Barclay, and D. C. Rees. 2002. Crystal structure of Escherichia coli MscS, a voltage-modulated and mechanosensitive channel. *Science.* 298:1582–1587.

Beckstein, O., and M. S. P. Sansom. 2003. Liquid-vapor oscillations of water in hydrophobic nanopores. *Proc. Natl. Acad. Sci. USA.* 100:7063–7068.

Berneche, S., and B. Roux. 2001. Energetics of ion conduction through the K^+ channel. *Nature.* 414:73–77.

Bezanilla, F., and E. Perozo. 2002. Force and voltage sensors in one structure. *Science.* 298:1562–1563.

Bloom, M. 1998. Evolution of membranes from a physics perspective. *Biol. Skr. Dan. Vid. Selsk.* 49:13–17.

Bond, P. J., J. D. Faraldo-Gómez, and M. S. P. Sansom. 2002. OmpA: a pore or not a pore? Simulation and modeling studies. *Biophys. J.* 83:763–775.

Brejc, K., W. J. van Dijk, R. V. Klaassen, M. Schuurmans, J. van der Oost, A. B. Smit, and T. K. Sixma. 2001. Crystal structure of an Ach-binding protein reveals the ligand-binding domain of nicotinic receptors. *Nature.* 411:269–276.

Brown, M. F. 1994. Modulation of rhodopsin function by properties of the membrane bilayer. *Chem. Phys. Lipids.* 73:159–180.

Chang, G., R. H. Spencer, A. T. Lee, M. T. Barclay, and D. C. Rees. 1998. Structure of the MscL homolog from Mycobacterium tuberculosis: a gated mechanosensitive ion channel. *Science.* 282:2220–2226.

Changeux, J. P. 1993. Chemical signaling in the brain. *Scien. Amer.* 1:58–62.

Corringer, P. J., S. Bertrand, J. L. Galzi, A. Devillers-Thiery, J. P. Changeux, and D. Bertrand. 1999. Mutational analysis of the charge selectivity filter of the alpha 7 nicotinic acetylcholine receptor. *Neuron.* 22:831–843.

Corringer, P. J., N. Le Novere, and J. P. Changeux. 2000. Nicotinic receptors at the amino acid level. *Annu. Rev. Pharmacol.* 40:431–458.

Darden, T., D. York, and L. Pedersen. 1993. Particle mesh Ewald: an N.log(N) method for Ewald sums in large systems. *J. Chem. Phys.* 98:10089–10092.

Doyle, D. A., J. M. Cabral, R. A. Pfuetzner, A. L. Kuo, J. M. Gulbis, S. L. Cohen, B. T. Chait, and R. MacKinnon. 1998. The structure of the potassium channel: molecular basis of K^+ conduction and selectivity. *Science.* 280:69–77.

Dutzler, R., E. B. Campbell, M. Cadene, B. T. Chait, and R. MacKinnon. 2002. X-ray structure of a ClC chloride channel at 3.0 A reveals the molecular basis of anion selectivity. *Nature.* 415:287–294.

Dzubiella, J., R. Allen, and J. P. Hansen. 2004. Electric field-controlled water permeation coupled to ion transport through a nanopore. *J. Chem. Phys.* 120:5001–5004.

Feller, S. E., and A. D. MacKerell Jr. 2000. An improved empirical potential energy function for molecular simulations of phospholipids. *J. Phys. Chem. B.* 104:7510–7515.

Frigyes, D., F. Alber, S. Pongor, and P. Carloni. 2001. Arginine-phosphate salt bridges in protein-DNA complexes: a Car-Parrinello study. *J. Mol. Struct.* 574:39–45.

Galzi, J. L., A. Devillers-Thiery, N. Hussy, S. Bertrand, J. P. Changeux, and D. Bertrand. 1992. Mutations in the channel domain of a neuronal nicotinic receptor convert ion selectivity from cationic to anionic. *Nature.* 359:500–505.

Grosman, C., M. Zhou, and A. Auerbach. 2000. Mapping the conformational wave of acetylcholine receptor channel gating. *Nature.* 403:773–776.

Hilgemann, D. W. 2004. Oily barbarians breach ion channel gates. *Science.* 304:223–224.

Hille, B. 1992. Ionic Channels of Excitable Membranes, 2nd ed. Sinauer Associates, Sunderland, MA.

Hummer, G., J. C. Rasaiah, and J. P. Noworyta. 2001. Water conduction through the hydrophobic channel of a carbon nanotube. *Nature.* 414:188–190.

Humphrey, W., A. Dalke, and K. Schulten. 1996. VMD — visual molecular dynamics. *J. Mol. Graph.* 14:33–38. http://www.ks.uiuc.edu/Research/vmd/

Itier, V., and D. Bertrand. 2001. Neuronal nicotinic receptors: from protein structure to function. *FEBS Lett.* 504:118–125.

Jiang, Y., A. Lee, J. Chen, M. Cadene, B. T. Chait, and R. MacKinnon. 2002a. The open pore conformation of potassium channels. *Nature.* 417:523–526.

Jiang, Y., A. Lee, J. Chen, M. Cadene, B. T. Chait, and R. MacKinnon. 2002b. Crystal structure and mechanism of a calcium-gated potassium channel. *Nature.* 417:515–522.

Jiang, Y., A. Lee, J. Chen, V. Ruta, M. Cadene, B. T. Chait, and R. MacKinnon. 2003a. X-ray structure of a voltage-dependent K^+ channel. *Nature.* 423:33–41.

Jiang, Y., V. Ruta, J. Chen, A. Lee, and R. MacKinnon. 2003b. The principle of gating charge movement in a voltage-dependent K^+ channel. *Nature.* 423:42–48.

Jorgensen, W. L., J. Chandrasekhar, J. D. Madura, R. W. Impey, and M. L. Klein. 1983. Comparison of simple potential functions for simulating liquid water. *J. Chem. Phys.* 79:926–935.

Karlin, A. 2002. Emerging structure of the nicotinic acetylcholine receptors. *Nat. Rev. Neurosci.* 3:102–114.

Karlin, A., and A. Akabas. 1995. Toward a structural basis for the function of the nicotinic acetylcholine receptors and their cousins. *Neuron.* 15:1231–1244.

Kelley, S. P., J. I. Dunlop, E. F. Kirkness, J. J. Lambert, and J. A. Peters. 2003. A cytoplasmic region determines single-channel conductance in 5–HT3 receptors. *Nature.* 424:321–324.

Killian, J. A. 2003. Synthetic peptides as models for intrinsic membrane proteins. *FEBS Lett.* 555:134–138.

Kuo, A., J. M. Gulbis, J. F. Antcliff, T. Rahman, E. D. Lowe, J. Zimmer, J. Cuthbertson, F. M. Ashcroft, T. Ezaki, and D. A. Doyle. 2003. Crystal structure of the potassium channel KirBac1.1 in the closed state. *Science.* 300:1922–1926.

Law, R. J., L. R. Forrest, K. M. Ranatunga, P. La Rocca, D. P. Tieleman, and M. S. P. Sansom. 2000. Structure and dynamics of the pore-lining helix of the nicotinic acetylcholine receptor: MD simulations in water, lipid bilayers, and transbilayer bundles. *Proteins.* 39:47–55.

Law, R. J., D. P. Tieleman, and M. S. P. Sansom. 2003. Pores formed by the nicotinic receptor M2δ peptide: a molecular dynamics simulations study. *Biophys. J.* 84:14–27.

Lear, J. D., Z. R. Wasserman, and W. F. DeGrado. 1988. Synthetic amphiphilic peptide models for protein ion channels. *Science.* 240:1177–1181.

Leite, J. F., and M. Cascio. 2001. Structure of ligand-gated ion channels: critical assessment of biochemical data supports novel topology. *Mol. Cell. Neurosci.* 17:777–792.

MacKerell, A. D. Jr., D. Bashford, M. Bellott, R. L. Dunbrack Jr., J. Evanseck, M. J. Field, S. Fischer, J. Gao, H. Guo, S. Ha, D. Joseph, L. Kuchnir, and others. 1998. All-atom empirical potential for molecular modeling and dynamics studies of proteins. *J. Phys. Chem. B.* 102:3586–3616.

MacKinnon, R. 2003. Potassium channels. *FEBS Lett.* 555:62–65.

Miyazawa, A., Y. Fujiyoshi, and N. Unwin. 2003. Structure and gating mechanism of the acetylcholine receptor pore. *Nature.* 423:949–955.

Montal, M. 1995. Design of molecular function: channels of communication. *Annu. Rev. Biophys. Biomol. Struct.* 24:31–57.

Montal, M., and S. J. Opella. 2002. The structure of the M2 channel-lining segment from the nicotinic acetylcholine receptor. *Biochim. Biophys. Acta.* 1565:287–293.

Oblatt-Montal, M., T. Iwamoto, J. M. Tomich, and M. Montal. 1993. Design, synthesis and functional characterization of a pentameric channel protein that mimics the presumed pore structure of the nicotinic cholinergic receptor. *FEBS Lett.* 320:261–266.

Oiki, S., W. Danho, V. Madison, and M. Montal. 1988. M2-δ, a candidate for the structure lining the ionic channel of the nicotinic cholinergic receptor. *Proc. Natl. Acad. Sci. USA.* 85:8703–8707.

Opella, S. J., F. M. Marassi, J. J. Gesell, A. P. Valente, Y. Kim, M. Oblatt-Montal, and M. Montal. 1999. Structures of the M2 channel-lining segments from nicotinic acetylcholine and NMDA receptors by NMR spectroscopy. *Nat. Struct. Biol.* 6:374–379.

Pandit, S. A., D. Bostick, and M. L. Berkowitz. 2003. Molecular dynamics simulation of a dipalmitoylphosphatidylcholine bilayer with NaCl. *Biophys. J.* 84:3743–3750.

Pashkov, V. S., I. V. Maslennikove, L. D. Tchikin, R. G. Efremov, V. T. Ivanov, and A. S. Arseniev. 1999. Spatial structure of the M2 transmembrane segment of the nicotinic acetylcholine receptor α-subunit. *FEBS Lett.* 457:117–121.

Pastor, R. W., R. M. Venable, and S. E. Feller. 2002. Lipid bilayers, NMR relaxation, and computer simulations. *Acc. Chem. Res.* 35:438–446.

Patra, M., M. Karttunen, M. Hyvonen, E. Falck, P. Lindqvist, and I. Vattulainen. 2003. Molecular dynamics simulations of lipid bilayers: major artifacts due to truncating electrostatic interactions. *Biophys. J.* 84:3636–3645.

Roux, B. 2002. Computational studies of the gramicidin channel. *Acc. Chem. Res.* 35:366–375.

Saiz, L., S. Bandyopadhyay, and M. L. Klein. 2002. Towards an understanding of complex biological membranes from atomistic molecular dynamics simulations. *Bioscience Rep.* 22:151–173.

Saiz, L., S. Bandyopadhyay, and M. L. Klein. 2004. Effect of the pore region of a transmembrane ion-channel on the physical properties of a simple membrane. *J. Phys. Chem. B*. 108:2608–2613.

Saiz, L., and M. L. Klein. 2002. Computer simulation studies of model biological membranes. *Acc. Chem. Res.* 35:482–489.

Sansom, M. S. P., and H. Weinstein. 2000. Hinges, swivels and switches: the role of prolines in signalling via transmembrane alpha-helices. *Trends Pharmacol. Sci.* 21:445–451.

Schlenkrich, M., J. Brickmann, A. D. MacKerell Jr., and M. Karplus. 1996. An empirical potential energy function for phospholipids: criteria for parameter optimization and applications. *In* Biological Membranes: A Molecular Perspective from Computation and Experiment. K. M. Merz and B. Roux, editors. Birkhauser, Boston. 31–82.

Stryer, L. 1995. Biochemistry, 4th ed. W. H. Freeman and Co., New York.

Tajkhorshid, E., P. Nollert, M. O. Jensen, L. J. W. Miercke, J. O'Connell, R. M. Stroud, and K. Schulten. 2002. Control of the selectivity of the aquaporin water channel family by global orientational tuning. *Science*. 296:525–530.

Tobias, D. J. 2001. Electrostatics calculations: recent methodological advances and applications to membranes. *Curr. Op. Struct. Bio.* 11:253–261.

Toyoshima, C., and N. Unwin. 1988. Ion channel of acetylcholine receptor reconstructed from images of postsynaptic membranes. *Nature*. 336:247–250.

Tuckerman, M. E., B. J. Berne, and G. J. Martyna. 1992. Reversible multiple time scale molecular dynamics. *J. Chem. Phys.* 97:1990–2001.

Tuckerman, M. E., D. A. Yarne, S. O. Samuelson, A. L. Hughes, and G. J. Martyna. 2000. Exploiting multiple levels of parallelism in molecular dynamics based calculations via modern techniques and software paradigms on distributed memory computers. *Comput. Phys. Commun.* 128: 333–376.

Unwin, N. 1993. Nicotinic acetylcholine receptor at 9 Å resolution. *J. Mol. Biol.* 229:1101–1124.

Unwin, N. 1995. Acetylcholine receptor channel imaged in the open state. *Nature.* 373:37–43.

Unwin, N. 2003. Structure and action of the nicotinic acetylcholine receptor explored by electron microscopy. *FEBS Lett.* 555:91–95.

Valiyaveetil, F. I., Y. F. Zhou, and R. MacKinnon. 2002. Lipids in the structure, folding, and function of the KcsA K^+ channel. *Biochemistry.* 41:10771–10777.

White, S. H., and M. C. Wiener. 1992. Structure of a fluid dioleoylphosphatidylcholine bilayer determined by joint refinement of x-ray and neutron diffraction data. III. Complete structure. *Biophys. J.* 61:434–447.

Zhong, Q. F., Q. Jiang, P. B. Moore, D. M. Newns, and M. L. Klein. 1998. Molecular dynamics simulation of a synthetic ion channel. *Biophys. J.* 74:3–10.

Zhong, Q. F., D. M. Newns, P. Pattnaik, J. D. Lear, and M. L. Klein. 2000. Two possible conducting states of the influenza A virus M2 ion-channel. *FEBS Lett.* 473:195–198.